A MEMS Coriolis Mass Flow Sensing System with Combined Drive and Sense Interface

A. C. de Oliveira[1,*], T. V. P. Schut[2], J. Groenesteijn[2,3], Q. Fan[1], R. J. Wiegerink[2] and K. A. A. Makinwa[1]
[1]Electronic Instrumentation Laboratory, Delft University of Technology, Delft, The Netherlands
[2]MESA+, University of Twente, Enschede, The Netherlands
[3]Bronkhorst High-Tech BV, Ruurlo, The Netherlands
[*]a.camposdeoliveira@tudelft.nl

***Abstract*—This paper describes an interface circuit for a MEMS Coriolis mass flow sensor that combines both drive and sense circuitry. The MEMS sensor consists of a suspended resonant tube, which is read-out by comb capacitors and driven into oscillation by current flowing through a drive coil in a magnet field. The interface circuit comprises a low-noise front-end that performs capacitance-to-voltage (C/V) conversion, and a drive-loop with automatic amplitude control. Drive motion can also be detected from the output of the front-end, allowing both drive and sense functions to be combined. The front-end is chopped to mitigate its $1/f$ noise. When implemented with commercial off-the-shelf (COTS) components, the proposed interface draws 250 mA from a single 5-V supply. Mass flow measurements with Nitrogen gas (N_2) show that the sensor's drive frequency drifts by less than 1 mHz (rms) per hour, while its zero stability is less than 2.6 mg/h during an 80s measurement.**

***Keywords*— MEMS, Coriolis, gyroscopic, mass flow, sensor interface.**

I. Introduction

Due to their low-cost and small size microelectromechanical systems (MEMS) form the basis of many mechanical sensors such as Coriolis mass flow sensors, accelerometers, and gyroscopes [1]–[5]. Traditionally, MEMS-based mass flow sensors have measured mass flow indirectly, e.g. by measuring fluid volume or heat capacity, and so are sensitive to fluid properties and ambient conditions, such as fluid temperature and pressure. Coriolis (or gyroscopic) mass flow sensors, however, are theoretically able to measure mass flow directly, independently of any fluid parameters, while providing both density and mass flow information [3].

Although several MEMS-based Coriolis mass flow sensors have been reported [1]–[3], not many dedicated interfaces have been developed. Such interfaces should perform two functions: 1) drive a fluid-carrying suspended tube into resonance, and 2) read out the resulting flow-dependent motion with high resolution. This paper presents a dedicated interface circuit for a MEMS-based Coriolis mass flow sensor [3] which combines both drive and sense functions while providing improved frequency (density) and phase (mass flow) stability compared to previous work [6], [7].

The rest of the paper is organized as follows. Section II describes the MEMS Coriolis mass flow sensor and its operation principle. The proposed drive and sense interface is discussed in Section III. The PCB implementation and measurement results are given in Section IV. Finally, Section V draws the conclusions.

II. MEMS Coriolis Mass Flow Sensor

The operating principle of the MEMS Coriolis mass flow sensor [3] is illustrated in Fig. 1. The flow to be sensed is passed through a MEMS sensing element, which consists of a silicon nitride resonating tube and two readout capacitors with which the motion of the tube can be sensed. In the presence of an external magnetic field (B), the tube can be driven at its twist mode resonance frequency ω_T by passing an AC-current through a metal coil deposited on top of the tube. When fluid flows through the channel, the resulting Coriolis force excites the tube's swing mode at the drive frequency (ω_T).

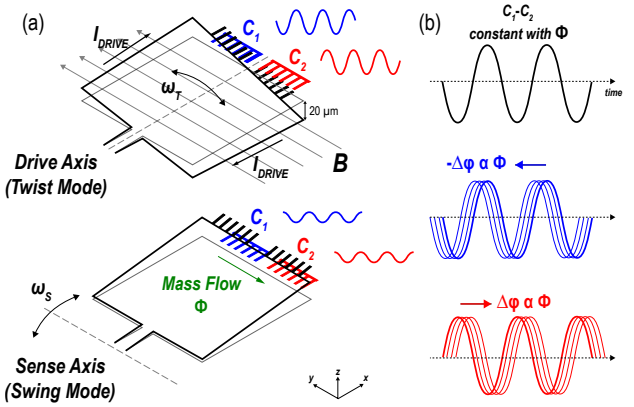

Fig. 1. MEMS Coriolis mass flow sensor (a) operation principle and (b) capacitive signals in the time-domain.

As shown in Fig. 1, each readout capacitor, C_1 and C_2, then senses a twist and a swing (Coriolis) component. The twist component can be expressed as

$$C_T = \hat{C}_T \sin(\omega_T t) \tag{1}$$

When mass flows through the tube, the swing mode is excited by the Coriolis force, resulting in a capacitance change given by

$$C_S = \hat{C}_S \cos(\omega_T t) \tag{2}$$

978-1-7281-1634-1/19/$31.00 ©2019 IEEE

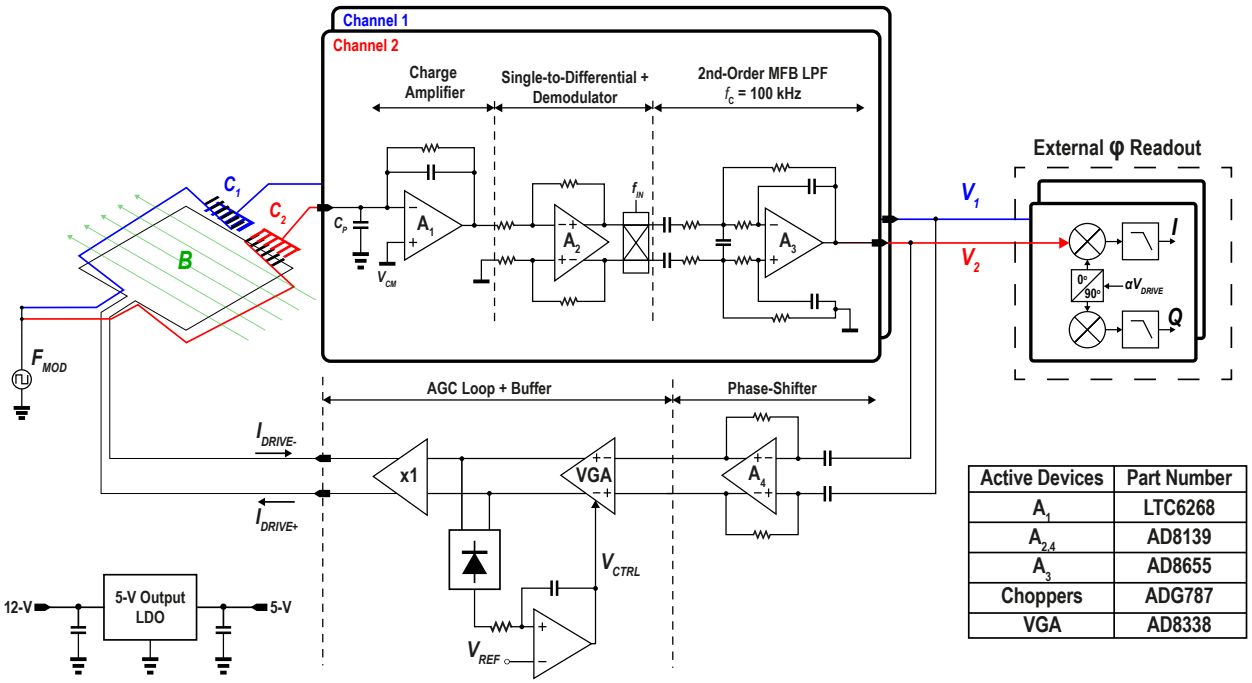

Active Devices	Part Number
A_1	LTC6268
$A_{2,4}$	AD8139
A_3	AD8655
Choppers	ADG787
VGA	AD8338

Fig. 2. Implementation of the proposed combined drive and sense paths.

where $\hat{C}_T$ and $\hat{C}_S$ are the twist and swing capacitance amplitudes, respectively. The composite capacitive signals can now be written as

$$C_1 = C_S - C_T = -\hat{C} \cdot \sin(\omega_T t - \varphi) \tag{3}$$

$$C_2 = C_S + C_T = \hat{C} \cdot \sin(\omega_T t + \varphi) \tag{4}$$

with $\hat{C} = \sqrt{\hat{C}_T^2 + \hat{C}_S^2}$. Through (3), (4) and trigometric identities, one can deduce that

$$\Delta\varphi = 2 \cdot \arctan\left(\frac{\hat{C}_S}{\hat{C}_T}\right) \approx 2 \cdot \left(\frac{\hat{C}_S}{\hat{C}_T}\right) \tag{5}$$

for small phase differences. This is proportional to the Coriolis force, and is thus a direct measure of mass flow. From (3) and (4), the difference between the two capacitive signals, C_1 and C_2, represents the drive (twist) motion, while their sum represents the sense (Coriolis/swing) motion. It is thus possible to detect both drive and sense motion using the same set of signals.

III. Combined Drive and Sense Interface

The proposed drive and sense interface is shown in Fig. 2. It consists of two capacitive readout channels, and a drive path with an automatic gain control (AGC) loop. The drive signal is applied to a metal coil realized on top of the resonating tube, while a separate metal trace is connected to the common terminal of the sense capacitors.

The capacitance-to-voltage conversion is performed by a charge-amplifier. The common terminals of the readout capacitors are driven by an external 20 V_{pp} square wave F_{MOD}, which modulates the motion-dependent signal (around $\omega_T \sim 3$ kHz) away from the amplifiers $1/f$ noise. F_{MOD} is set to 1 MHz, which is higher than the amplifier's $1/f$ corner, and is also higher than the sensor's parasitic resonance frequencies.

After a single-ended to differential conversion, the resulting amplitude modulated signal is demodulated by a passive mixer (chopper), which simultaneously up-modulates the amplifier's $1/f$ noise. A 2nd-order low-pass filter (LPF) filters out the chopping harmonics. To block the offset of the previous stages, capacitors (10-µF) are added before the LPF. A 100 kHz LP cut-off frequency was chosen as a compromise between the need to reject the up-modulated noise at the harmonics of F_{MOD} and the need to minimize the extra phase-shift added to the motion-dependent signal. The input-referred noise of each channel is mainly determined by the amplifier's thermal noise, boosted by the input capacitance C_p formed by the sensor, PCB and interconnect capacitances.

The phase difference between the readout (V_1 and V_2) and drive (V_{DRIVE}) is detected with the help of two SR865A lock-in amplifiers. To avoid introducing extra phase errors, their reference signal (αV_{DRIVE}) is derived from the difference between the readout signals.

To cancel the effect of mass flow, the drive signal is also generated from the difference of the two readout channels (Fig. 1). This is applied to a differentiator, which provides 90^o phase-shift, thus ensuring that the drive-loop meets the requirements for oscillation. Its output signal is then amplified by a variable-gain amplifier (VGA), regulated to a fixed amplitude that can be adjusted via V_{REF}.This is done to control the self-heating caused by the large currents (∼10 mA) flowing through the drive coil, and to prevent the tube from operating

in its mechanically non-linear region, both of which would impact the sensor's long-term stability. In this work, a drive amplitude of 2 V is used, which corresponds to a 20 µm displacement at the corners of the sensor (Fig. 1(a)).

IV. PCB Implementation and Measurement Results

The combined drive and sense interface is implemented using the commercial off-the-shelf (COTS) components tabulated in Fig. 2. The PCB and MEMS sensing element are shown in Fig. 3. The total system consists of a main PCB, with the interface circuitry and two fluidic connectors, and a small PCB (center) to which the MEMS Coriolis mass flow sensor chip is bonded. The whole system consumes 250 mA from a single 5-V supply.

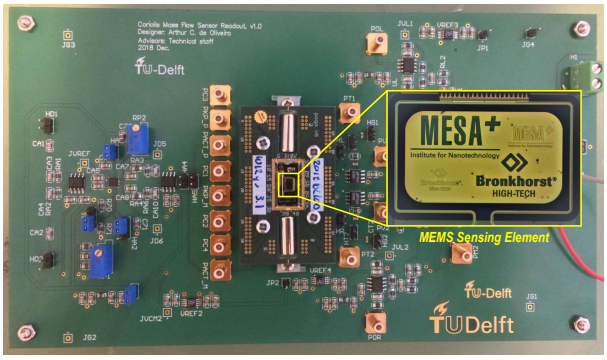

Fig. 3. PCB implementation photo and the MEMS Coriolis mass flow sensor micrograph.

Mass flow measurements are performed using Nitrogen gas (N_2), which is applied to the sensor via 3D-printed fluidic connectors mounted below the PCB. The N_2 mass flow is controlled by an external mass flow controller at the sensor's inlet, while a pressure controller at the sensor's outlet regulates the pressure drop across the sensor.

The phase difference between the readout signals with respect to N_2 mass flow is shown in Fig. 4, where the maximum mass flow applied is about 0.75 g/h with a 75 mg/h step. To verify that the sensor exhibits no hysteresis, the presented measurements include both increasing and decreasing phase-to-mass flow responses, with each point representing the average of a 30s measurement. The differential phase readout achieves 4.7 °/(g/h) mass flow sensitivity (S_Φ) which, as expected, is about 2× larger than that of single-ended signals (φ_1 and φ_2). No significant loss in sensitivity was observed due to mismatch between the channels.

Since all mass flow sensors require calibration, one of the most important specifications of such sensors is their stability (or repeatability). The stability of a sensor is evaluated by observing how its output under zero flow rate drifts as a function of time, i.e. its zero stability (ZS). In this work, we are interested in the sensor's phase (mass flow) and drive frequency (density) stability. These measurements are presented in Fig. 5. The proposed system shows a ZS of 2.6 mg/h (1-Hz bandwidth) for an 80s measurement, which

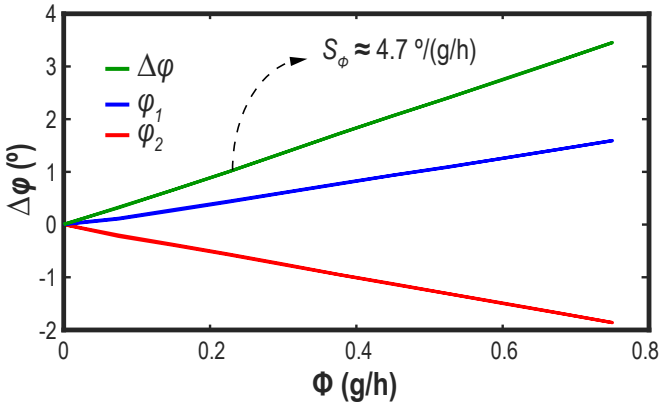

Fig. 4. Measurements of the phase response for N_2 and the sensor's mass flow sensitvity.

is also a measure of its mass flow resolution. Even though this is less than the 10 mg/h ZS achieved by a state-of-the-art commercially-available Coriolis mass flow sensor [8], there is room for improvement. This is because the phase stability of the sensor is still dominated by noise sources other than its interface electronics.

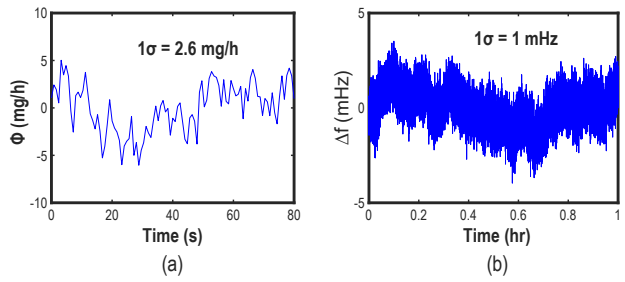

Fig. 5. Stability measurements for (a) mass flow and (b) frequency.

The drift in the sensors driving frequency (ω_T ~3 kHz) is shown in Fig. 5(b) over one full hour. It is less than 1 mHz (rms), which is about 80× less than the drift achieved by the drive loops of similar Coriolis mass flow sensors [6], [7].

V. Conclusion

A MEMS Coriolis mass flow sensing system with combined drive and sense interface circuitry has been presented. This is based on the observation that the output of its capacitive readout circuitry contain both the drive and the Coriolis signals. Mass flow measurements with N_2 show that the sensor achieves a mass flow sensitivity of 4.7 °/(g/h) with a zero stability of 2.6 mg/h. The drive frequency stability is more than 80× better than that achieved by the drive loops of similar Coriolis mass flow sensors. These results demonstrate that capacitive readout is well suited for the detection of both drive and sense motion.

REFERENCES

[1] P. Enoksson, G. Stemme, and E. Stemme, "A Silicon Resonant Sensor Structure for Coriolis Mass-Flow Measurements," *Journal of Microelectromechanical Systems*, vol. 6, no. 2, pp. 119–125, June 1997.

[2] R. Smith, D. R. Sparks, D. Riley, and N. Najafi, "A MEMS-Based Coriolis Mass Flow Sensor for Industrial Applications," *IEEE Transactions on Industrial Electronics*, vol. 56, no. 4, pp. 1066–1071, April 2009.

[3] D. Alveringh, R. J. Wiegerink, and J. C. Lötters, "Integrated Pressure Sensing Using Capacitive Coriolis Mass Flow Sensors," *Journal of Microelectromechanical Systems*, vol. 26, no. 3, pp. 653–661, June 2017.

[4] Y. Zhao, J. Zhao, X. Wang, G. M. Xia, A. P. Qiu, Y. Su, and Y. P. Xu, "A Sub-μg Bias-Instability MEMS Oscillating Accelerometer With an Ultra-Low-Noise Read-Out Circuit in CMOS," *IEEE Journal of Solid-State Circuits*, vol. 50, no. 9, pp. 2113–2126, Sep. 2015.

[5] M. Marx, S. Rombach, S. Nessler, D. De Dorigo, and Y. Manoli, "A 141-μW High-Voltage MEMS Gyroscope Drive Interface Circuit Based on Flying Capacitors," *IEEE Journal of Solid-State Circuits*, vol. 54, no. 2, pp. 511–523, Feb 2019.

[6] J. Groenesteijn, M. Dijkstra, T. Lammerink, J. C. Lötters, and R. Wiegerink, "A compact micro Coriolis mass flow sensor with flow bypass for a monopropellant micro propulsion system," *2nd Conference on MicroFluidic Handling Systems (MFHS)*, Oct 2014.

[7] D. Alveringh, T. Schut, R. Wiegerink, and J. C. Lötters, "Coriolis mass flow and density sensor actuation using a phase-locked loop," *3nd Conference on MicroFluidic Handling Systems (MFHS)*, Oct 2017.

[8] Bronkhorst, "mini CORI-FLOW™ ML120V21 datasheet," 2018.